

# Light mesons from JPAC+COMPASS analyses

Misha Mikhasenko

Joint Physics Analysis Center,  
COMPASS @ CERN,  
CERN, Switzerland

PsiPhi 2019  
Adkademgorodok

27.02.2019



# Contents

## 1 Introduction

- JPAC Collaboration
- Challenges of hadron spectroscopy

## 2 $\eta^{(\prime)}\pi$ analyses

- COMPASS data
- Method to extract resonance properties
- Coupled-channel analysis

## 3 Three-pions physics

- COMPASS PWA
- Deck mechanism
- Data for the  $1^{++}$  sector
- Analysis of  $\tau$ -data

## 4 Summary

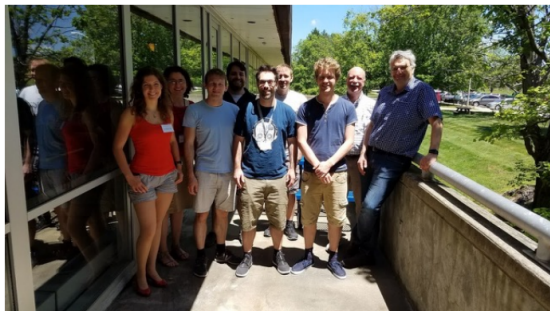
# Introduction

# Joint Physics Analysis Center

[collage by Vincent Mathieu]

**Emilie Passemar** **Andrew Jackura** **Nathan Sherrill** **Tim Londergan**  
 Indiana U. Indiana U. Indiana U. Indiana U.

**Astrid Hiller Blin** **Misha Mikhasenko VM** **Jannes Nys** **Adam Szczepaniak**  
 Mainz U. Bonn U. JLab Ghent U. Indiana U.



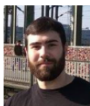
**Cesar Fernández-Ramírez**  
UNAM



**Alessandro Pilloni**  
JLab → ECT\*



**Łukasz Bibrzycki**  
Cracow P. U.



**Arkaitz Rodas Bilbao**  
Madrid U.



**Viktor Mokeev**  
JLab

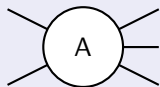


**Miguel Albaladejo**  
JLab

# JPAC effort

Collaboration of theoreticians and experimentalists

## Amplitude analysis

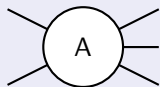


- Writing amplitudes using general QFT constraints
- Analysis of experimental data
- Analytic continuation, pole search

# JPAC effort

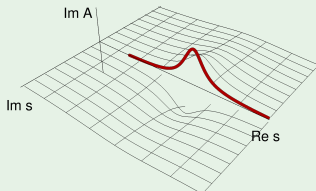
Collaboration of theoreticians and experimentalists

## Amplitude analysis



- Writing amplitudes using general QFT constraints
- Analysis of experimental data
- Analytic continuation, pole search

## General properties of the scattering amplitude



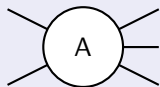
Analyticity + Unitary + Crossing symmetry

- Scattering amplitude is an analytic function in  $s = E^2$  complex plane,
- The Real axis  $\rightarrow$  physical world,
- Resonances = poles of the unphysical sheet.

# JPAC effort

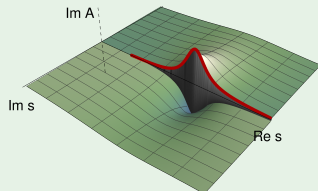
Collaboration of theoreticians and experimentalists

## Amplitude analysis



- Writing amplitudes using general QFT constraints
- Analysis of experimental data
- Analytic continuation, pole search

## General properties of the scattering amplitude



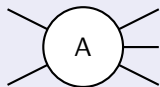
Analyticity + Unitary + Crossing symmetry

- Scattering amplitude is an analytic function in  $s = E^2$  complex plane,
- The Real axis  $\rightarrow$  physical world,
- Resonances = poles of the unphysical sheet.

# JPAC effort

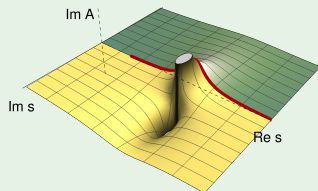
Collaboration of theoreticians and experimentalists

## Amplitude analysis



- Writing amplitudes using general QFT constraints
- Analysis of experimental data
- Analytic continuation, pole search

## General properties of the scattering amplitude



Analyticity + Unitary + Crossing symmetry

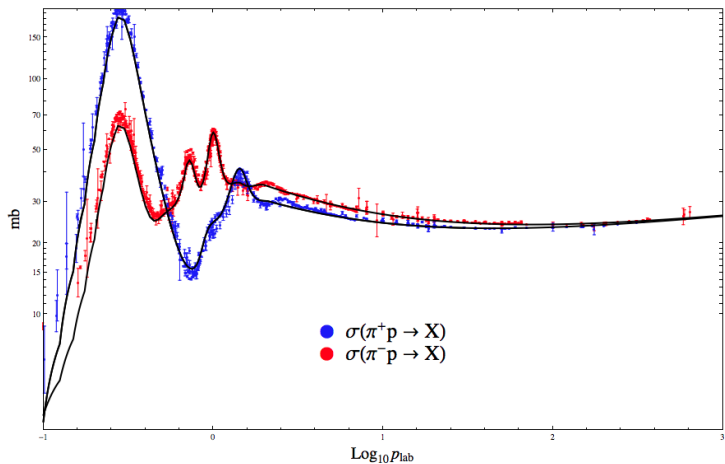
- Scattering amplitude is an analytic function in  $s = E^2$  complex plane,
- The Real axis  $\rightarrow$  physical world,
- Resonances = poles of the unphysical sheet.



# Two regimes of scattering

Hadronic duality

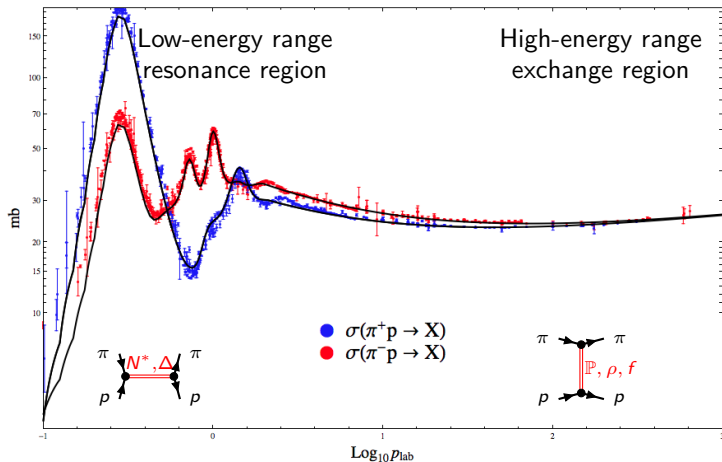
[V.Mathieu, et al., PRD92 (2015), 074004]



# Two regimes of scattering

Hadronic duality

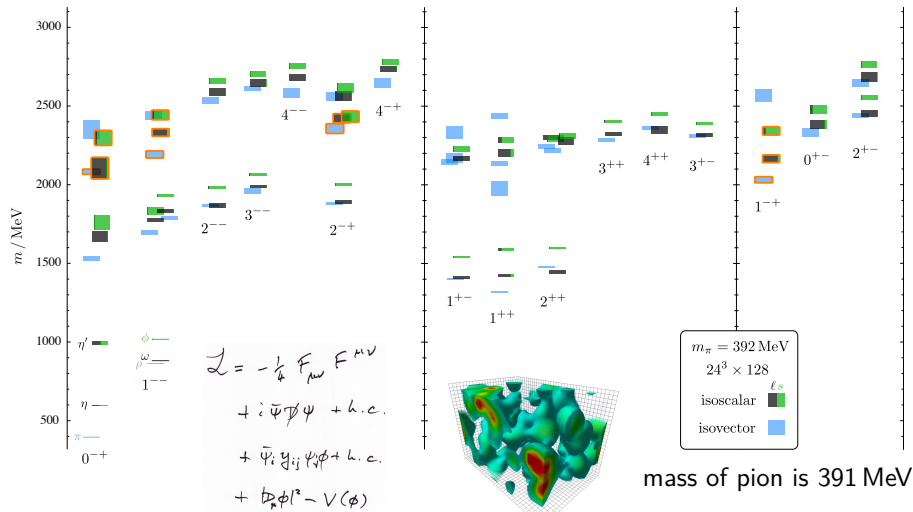
[V.Mathieu, et al., PRD92 (2015), 074004]



# Hadronic excitations

Results of lattice QCD

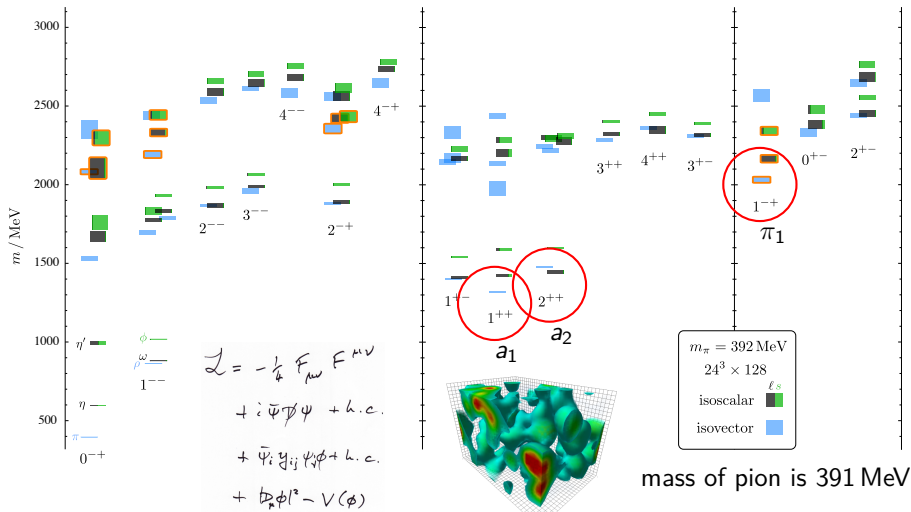
[Dudek et al., PRD 88, 094505 (2013)]



# Hadronic excitations

Results of lattice QCD

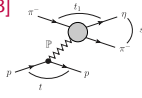
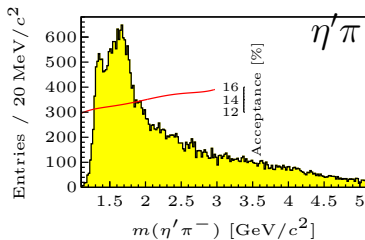
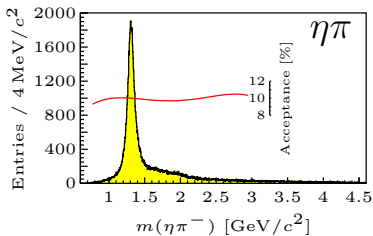
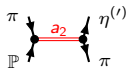
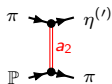
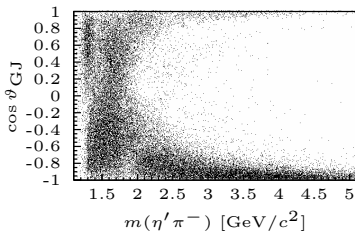
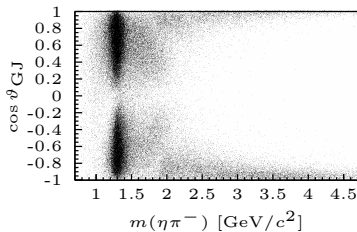
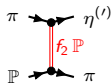
[Dudek et al., PRD 88, 094505 (2013)]



# $\eta^{(\prime)}\pi$ analyses

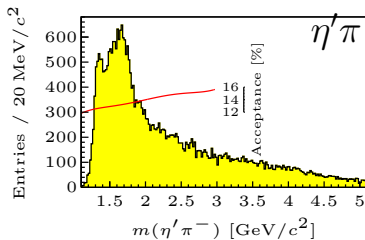
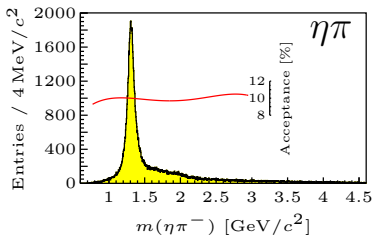
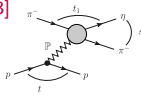
$\eta\pi$  vs  $\eta'\pi$  at COMPASS

[[COMPASS) PLB 740 (2015) 303]

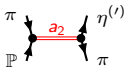
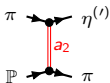
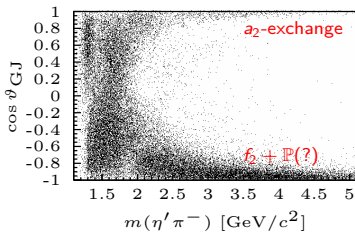
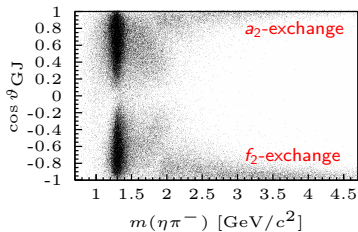
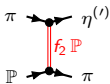
Resonance  
production $\eta$ -forward  
production $\pi$ -forward  
production
 $\eta^{(\prime)}(0^-)\pi(0^-)$ ,  $J^{PC} = L^{P+} \Rightarrow \cos\theta_{GJ}$  asymmetry  $\Rightarrow$  exotic waves!

$\eta\pi$  vs  $\eta'\pi$  at COMPASS

[[COMPASS) PLB 740 (2015) 303]



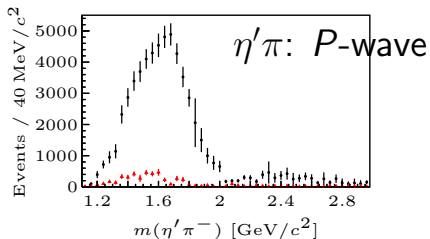
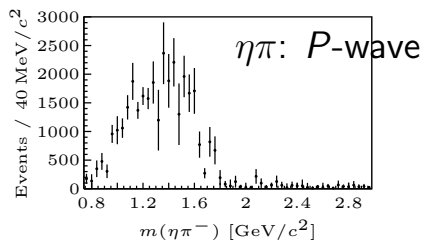
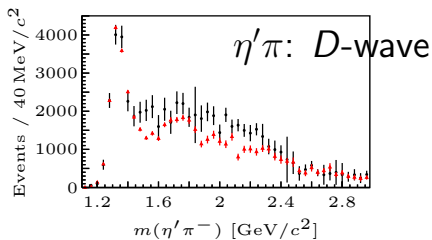
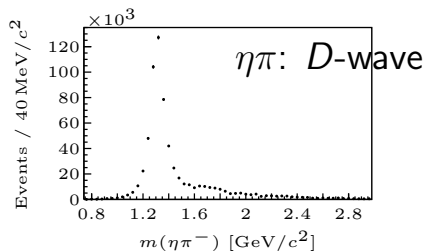
Resonance production

 $\eta$ -forward production $\pi$ -forward production
 $\eta^{(\prime)}(0^-)\pi(0^-)$ ,  $J^{PC} = L^{P+} \Rightarrow \cos\theta_{GJ}$  asymmetry  $\Rightarrow$  exotic waves!

# $\eta^{(\prime)}\pi$ partial wave analysis

Two-main contribution:  $P$ - and  $D$ -waves

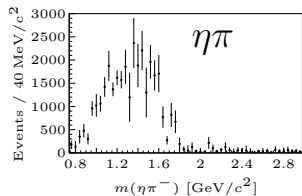
[(COMPASS) PLB 740 (2015) 303]





# PDG status: exotic $\pi_1$ states

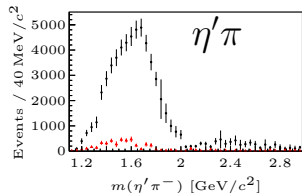
## Two candidates



$$\pi_1(1400) \quad I^G(J^{PC}) = 1^-(1^{-+})$$

See also the mini-review under non- $q\bar{q}$  candidates in PDG 2006, Journal of Physics G33 1 (2006).

$\pi_1(1400)$ MASS	$1354 \pm 25$ MeV (S = 1.8)	
$\pi_1(1400)$ WIDTH	$330 \pm 35$ MeV	
<b>Decay Modes</b>		
Mode	Fraction ( $\Gamma_i / \Gamma$ )	Scale Factor/ P Conf. Level (MeV/c)
$\Gamma_1$ $\eta\pi^0$	seen	557
$\Gamma_2$ $\eta\pi^-$	seen	556
$\Gamma_3$ $\eta'\pi$		318



$$\pi_1(1600) \quad I^G(J^{PC}) = 1^-(1^{-+})$$

$\pi_1(1600)$ MASS	$1662^{+8}_{-9}$ MeV	
$\pi_1(1600)$ WIDTH	$241 \pm 40$ MeV (S = 1.4)	
<b>Decay Modes</b>		
Mode	Fraction ( $\Gamma_i / \Gamma$ )	Scale Factor/ P Conf. Level (MeV/c)
$\Gamma_1$ $\pi\pi\pi$	seen	803
$\Gamma_2$ $\rho^0\pi^-$	seen	641
$\Gamma_3$ $f_2(1270)\pi^-$	not seen	318
$\Gamma_4$ $b_1(1235)\pi$	seen	357
$\Gamma_5$ $\eta'(958)\pi$	seen	543
$\Gamma_6$ $f_1(1285)\pi$	seen	314

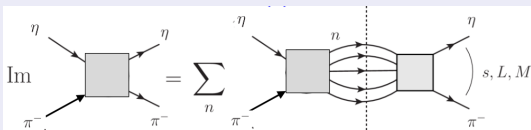
# Amplitude for $\eta\pi$ production [A.Jackura,MM,A.Pilloni,et al. (JPAC-COMPASS),

PLB779, 464-472]

$N$ -over- $D$  method

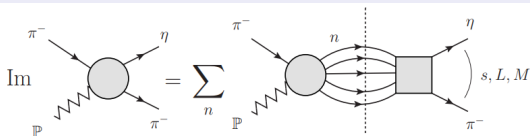
Scattering amplitude:  $\eta\pi \rightarrow \eta\pi$ ,  $D$ -wave

$$T = \frac{N(s)}{D(s)}$$



Production amplitude:  $\pi\mathbb{P} \rightarrow \eta\pi$ ,  $D$ -wave

$$a = \frac{n(s)}{D(s)}$$

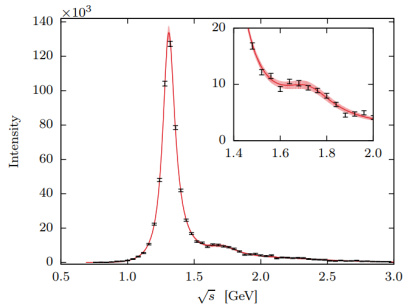


- $D(s)$  is universal, has only the right-hand cut.
- $N(s)$  and  $n(s)$  have the left-hand cut only (exchanges)

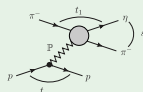
# Tensor mesons ( $J^{PC} = 2^{++}$ )

Advanced  $\eta\pi$  analysis

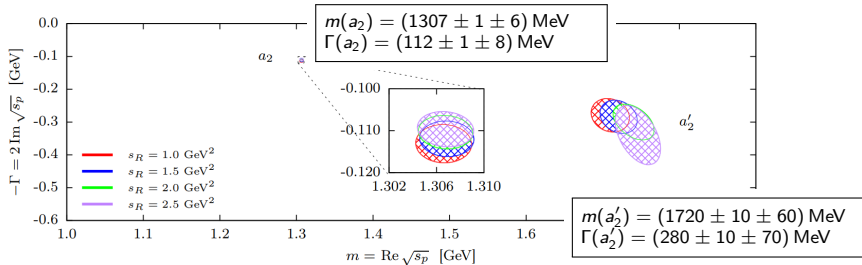
[A.Jackura,MM,A.Pilloni,et al. (JPAC-COMPASS), PLB779, 464-472]



## Single channel: $\eta\pi$ $D$ -wave



- Elastic unitarity
- Two CDD-poles



# Coupled-channel amplitude [A.Rodas,A.Pilloni,MM,et al. (JPAC), PRL122 (2019)]

Scattering amplitude:  $\eta^{(\prime)}\pi \rightarrow \eta^{(\prime)}\pi$ ,  $P/D$ -waves

$$T = \frac{N(s)}{D(s)}$$

$$\rho N_{ki}^J(s') = \delta_{ki} \frac{(p_{\eta^{(\prime)}\pi} \sqrt{s}/2)^{2J+1}}{(s' + s_L)^{2J+1+\alpha}},$$

- 2  $K$ -matrix pole for  $D$ -wave
- 1  $K$ -matrix pole for  $P$ -wave

$$D_{ki}^J(s) = [K^J(s)^{-1}]_{ki} - \frac{s}{\pi} \int_{s_k}^{\infty} ds' \frac{\rho N_{ki}^J(s')}{s'(s' - s - i\epsilon)}$$

Production amplitude:  $\pi\mathbb{P} \rightarrow \eta^{(\prime)}\pi$ ,  $P/D$ -waves

$$a = \frac{n(s)}{D(s)}$$

$$a_i^J(s) = q^{J-1} p_i^J \sum_k n_k^J(s) [D^J(s)^{-1}]_{ki}$$

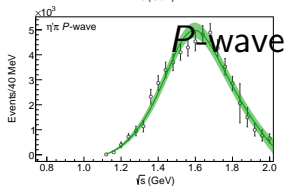
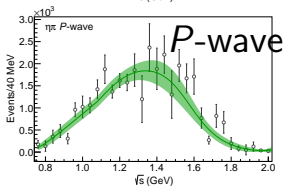
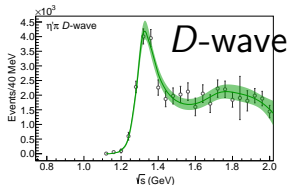
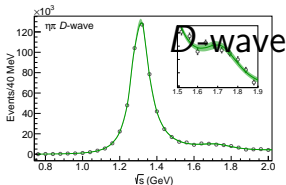
- left poles to model unknown production function  $n(s)$

- $D(s)$  has only the right-hand cut.
- $N(s)$  and  $n(s)$  have the left-hand cut only (exchanges)

# Fit to the data

[A.Rodas,A.Pilloni,MM,et al. (JPAC), PRL122 (2019)]

$\chi^2/\text{ndf} = 162/122$ , the band -  $2\sigma$  bootstrap error

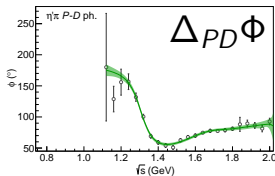
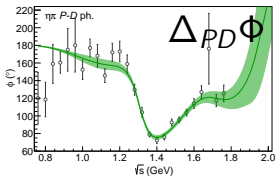


## D-wave difference

- Kinematics  
( $m_{\eta'} > m_{\eta}$ )
- ⇒ Same amplitude.

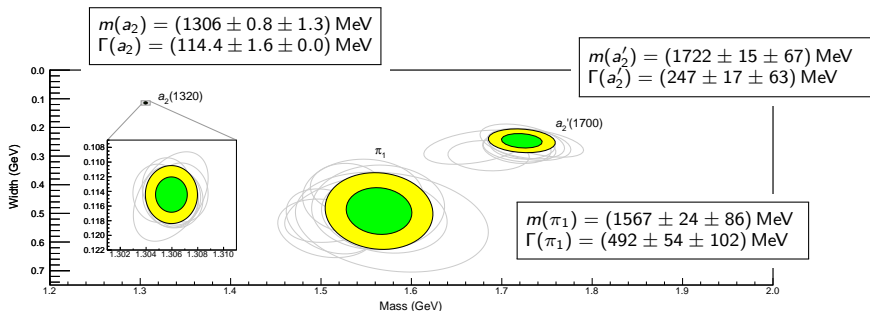
## P-wave difference

- production mechanism
- + kinematics.



## Results: pole positions

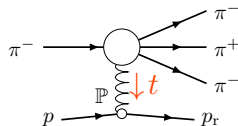
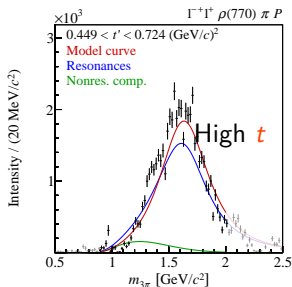
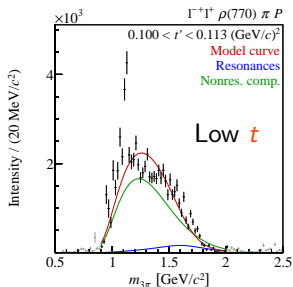
[A.Rodas,A.Pilloni,MM,et al. (JPAC), PRL122 (2019)]



- Change parametrization of the denominator  $\rho N_{ki}^J(s') = \delta_{ki} \frac{(p_{\eta^{(\prime)}\pi} \sqrt{s}/2)^{2J+1}}{(s'+s_L)^{2J+1+\alpha}}$ ,
  - ▶  $s_R = 1 \text{ GeV} \rightarrow 0.8, 1.8 \text{ GeV}$ .
  - ▶  $\alpha = 2 \rightarrow 1 \text{ GeV}$ .
  - ▶ Different function,  $\rho N_{ki}^J(s') = \delta_{ki} Q_J(z_{s'}) s'^{-\alpha} \lambda^{-1/2}(s', m_{\eta^{(\prime)}}^2, m_{\pi}^2)$
- Change of parameters in the numerator  $n(s)$ 
  - ▶ Effective transferred momentum  $t_{\text{eff}} = -0.1 \text{ GeV}^2 \rightarrow -0.5 \text{ GeV}^2$ .
  - ▶ Order of the polynomial 3rd-order  $\rightarrow$  4th-order.

# Same $\pi_1$ as in $3\pi$ ?

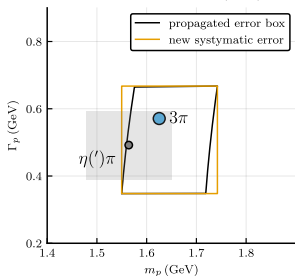
[See a talk of B.Ketzer, afternoon]



The COMPASS fit:

- Signal by BW amplitude
- Flexible background

Pole parameters of  $\pi_1(1600)$



Consistent results on  $\pi_1(1600)$  pole:

- $\rho\pi$  Breit-Wigner parameters  
 $\Rightarrow$  pole position
- $\eta^{(\prime)}\pi$  systematic margins

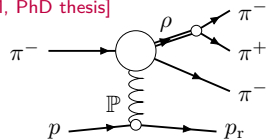
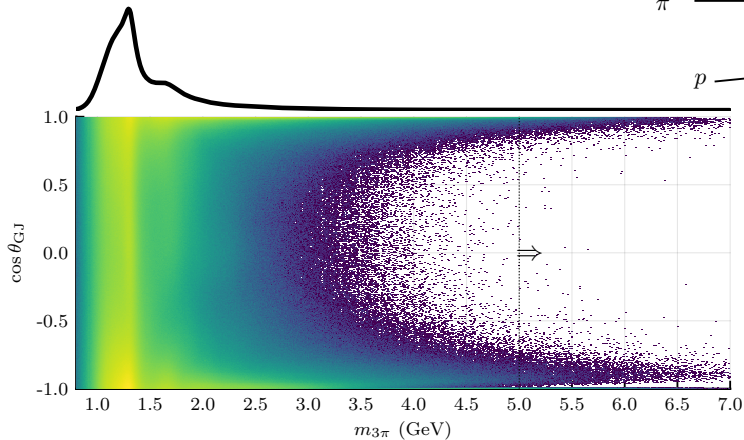
# Three-pions physics



# Diffractive production of $3\pi$ off proton target

Forward-background scattering

[COMPASS data, MM, PhD thesis]

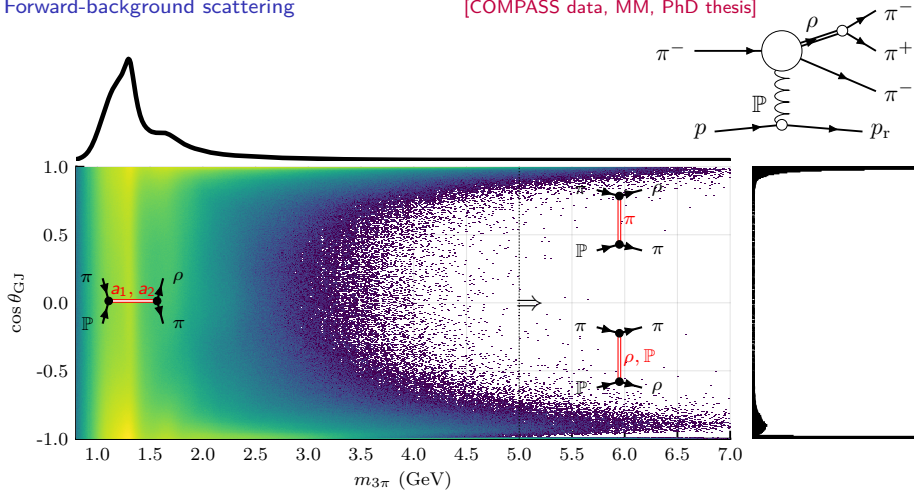


The high-energy exchange processes penetrate to the low energy and make resonance characterization difficult

# Diffractive production of $3\pi$ off proton target

Forward-background scattering

[COMPASS data, MM, PhD thesis]

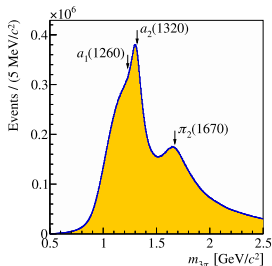


The high-energy exchange processes penetrate to the low energy and make resonance characterization difficult

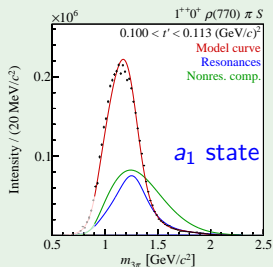
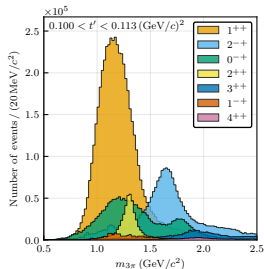
# Three-pion resonances

[see talk by D.Ryabchikov, afternoon]

COMPASS PWA [PRD95 (2017) 032004]



Partial Wave Analysis →



COMPASS Fit:

- Signal by BW amplitude  $\sim 50\%$
- Background  $\sim 50\%$

$$m_{a_1}^{(BW)} = (1299_{-28}^{+12}) \text{ MeV,}$$

$$\Gamma_{a_1}^{(BW)} = (380 \pm 80) \text{ MeV.}$$

Large uncertainty due to unknown background.

# Model for the forward scattering

[MM, A.Jackura (JPAC) in preparation]

Deck effect

$$= (T_{\pi_1 \rho})_{\lambda \lambda'} \frac{1}{m_\pi^2 - t_1} T_{\pi_2 \pi_3} \quad (1)$$

- Two diagrams ( $\pi^-$  symmetrization)

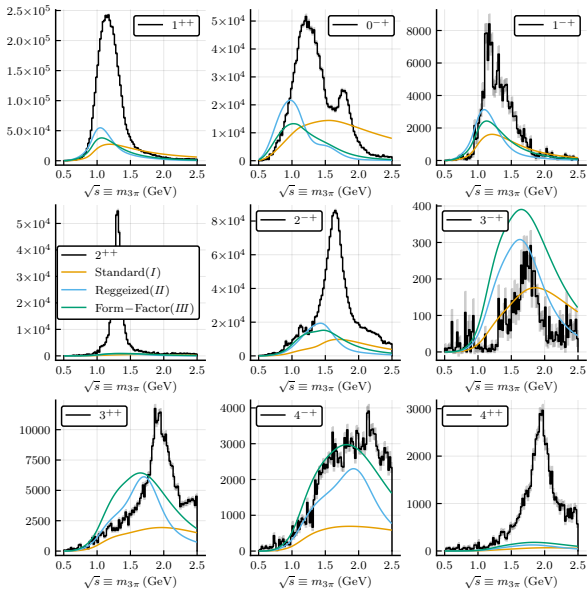
$$\mathcal{B}_{\lambda \lambda'} = \mathcal{B}_{\lambda \lambda'}^{(1)} + \mathcal{B}_{\lambda \lambda'}^{(3)}$$

- High energy  $p\pi$  scattering
- $\pi\pi$  scattering dominated by resonances in lower partial waves
  - ▶ Relative strength of  $S$ ,  $P$ ,  $D$ -waves is controlled by unitarity

$$\mathcal{B}^{(1)} = s_{\pi\rho} F(t) \frac{\text{FF}(t_1)}{m_\pi^2 - t_1} \left[ \frac{2}{3} t^{(\sigma_1, f_0)}(\sigma_1) + 3 t^{(\rho)}(\sigma_1, t_1) P_1(\cos \theta_{\pi\pi}) + \frac{10}{3} t^{(f_2)}(\sigma_1, t_1) P_2(\cos \theta_{\pi\pi}) \right].$$

# Comparison with the COMPASS data

[MM PhD thesis]



Pion propagator:

- Standard Deck

$$\frac{1}{m_{\pi}^2 - t_1},$$

- Regge Deck

$$\frac{e^{-i\pi\alpha(t_1)/2}}{m_{\pi}^2 - t_1} \left( \frac{s' - u'}{2s_{\text{Sc}}} \right)^{\alpha(t_1)}$$

- Form-factored Deck

$$\frac{e^{bt_1}}{m_{\pi}^2 - t_1},$$

$a_1(1260)$  state – isospin partner of  $\rho$  $a_1(1260)$  WIDTH[INSPIRE search](#)

VALUE (MeV)	EVTS	DOCUMENT ID	TECN	COMMENT
<b>250 to 600</b>	<b>OUR ESTIMATE</b>			
<b>389 ± 29</b>	<b>OUR AVERAGE</b>	Error includes scale factor of 1.3.		
430 ± 24 ± 31		<a href="#">DARGENT</a> 2017	RVUE	$D^0 \rightarrow \pi^- \pi^+ \pi^- \pi^+$
367 ± 9 <sup>+28</sup> <sub>-25</sub>	420k	<a href="#">ALEKSEEV</a> 2010	COMP	$190 \pi^- \rightarrow \pi^- \pi^- \pi^+ P_b'$
••• We do not use the following data for averages, fits, limits, etc. •••				
410 ± 31 ± 30		<a href="#">1 AUBERT</a> 2007AU	BABR	$10.6 e^+ e^- \rightarrow \rho^0 \rho^\pm \pi^\mp \gamma$
520 - 680	6360	<a href="#">2 LINK</a> 2007A	FOCS	$D^0 \rightarrow \pi^- \pi^+ \pi^- \pi^+$
480 ± 20		<a href="#">3 GOMEZ-DUMM</a> 2004	RVUE	$\tau^+ \rightarrow \pi^+ \pi^+ \pi^- \nu_\tau$
580 ± 41	90k	<a href="#">SALVINI</a> 2004	OBLX	$\bar{p} p \rightarrow 2 \pi^+ 2 \pi^-$
460 ± 85	205	<a href="#">4 DRUTSKOY</a> 2002	BELL	$B^{(*)} K^- K^0$
814 ± 36 ± 13	37k	<a href="#">5 ASNER</a> 2000	CLE2	$10.6 e^+ e^- \rightarrow \tau^+ \tau^-$ , $\tau^- \rightarrow \pi^- \pi^0 \pi^0 \nu_\tau$

$a_1(1260)$  state – isospin partner of  $\rho$  $a_1(1260)$  WIDTH[INSPIRE search](#)

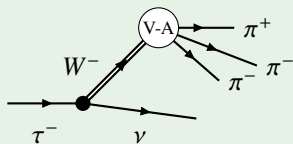
VALUE (MeV)	EVTS	DOCUMENT ID	TECN	COMMENT
250 to 600				<b>OUR ESTIMATE</b>
389 ± 29				<b>OUR AVERAGE</b> Error includes scale factor of 1.3.
430 ± 24 ± 31		DARGENT 2017	RVUE	$D^0 \rightarrow \pi^- \pi^+ \pi^- \pi^+$
367 ± 9 <sup>+28</sup> <sub>-25</sub>	420k	ALEKSEEV 2010	COMP	$190 \pi^- \rightarrow \pi^- \pi^- \pi^+ P_b'$
••• We do not use the following data for averages, fits, limits, etc. •••				
410 ± 31 ± 30		1 AUBERT 2007AU	BABR	$10.6 e^+ e^- \rightarrow \rho^0 \rho^\pm \pi^\mp \gamma$
520 - 680	6360	2 LINK 2007A	FOCS	$D^0 \rightarrow \pi^- \pi^+ \pi^- \pi^+$
480 ± 20		3 GOMEZ-DUMM 2004	RVUE	$\tau^+ \rightarrow \pi^+ \pi^+ \pi^- \nu_\tau$
580 ± 41	90k	SALVINI 2004	OBLX	$\bar{p} p \rightarrow 2 \pi^+ 2 \pi^-$
460 ± 85	205	4 DRUTSKOY 2002	BELL	$B^{(*)} K^- K^0$
814 ± 36 ± 13	37k	5 ASNER 2000	CLE2	$10.6 e^+ e^- \rightarrow \tau^+ \tau^-$ , $\tau^- \rightarrow \pi^- \pi^0 \pi^0 \nu_\tau$

$a_1(1260)$  state – isospin partner of  $\rho$  $a_1(1260)$  WIDTH

INSPIRE search

VALUE (MeV)	EVTS	DOCUMENT ID	TECN	COMMENT
250 to 600	<b>OUR ESTIMATE</b>			
389 ± 29	<b>OUR AVERAGE</b> Error includes scale factor of 1.3.			
430 ± 24 ± 31		DARGENT 2017	RVUE	$D^0 \rightarrow \pi^- \pi^+ \pi^- \pi^+$
367 ± 9 <sup>+28</sup> <sub>-25</sub>	420k	ALEKSEEV 2010	COMP	190 $\pi^- \rightarrow \pi^- \pi^- \pi^+ Pb'$
... We do not use the following data for averages, fits, limits, etc. ...				
410 ± 31 ± 30		1 AUBERT 2007AU	BABR	10.6 $e^+ e^- \rightarrow \rho^0 \rho^\pm \pi^\mp \gamma$
520 - 680	6360	2 LINK 2007A	FOCS	$D^0 \rightarrow \pi^- \pi^+ \pi^- \pi^+$
480 ± 20		3 GOMEZ-DUMM 2004	RVUE	$\tau^+ \rightarrow \pi^+ \pi^+ \pi^- \nu_\tau$
580 ± 41	90k	SALVINI 2004	OBLX	$\bar{p} p \rightarrow 2 \pi^+ 2 \pi^-$
460 ± 85	205	4 DRUTSKOY 2002	BELL	$B^{(*)} K^- K^0$
814 ± 36 ± 13	37k	5 ASNER 2000	CLE2	10.6 $e^+ e^- \rightarrow \tau^+ \tau^-$ , $\tau^- \rightarrow \pi^- \pi^0 \pi^0 \nu_\tau$

$$\tau^- \rightarrow \pi^- \pi^+ \pi^- \nu$$



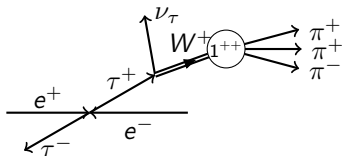
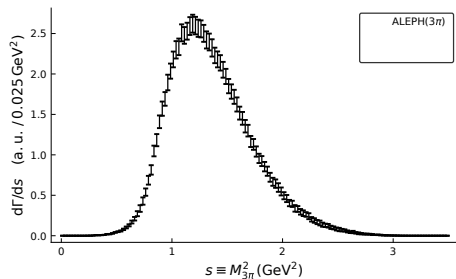
- V-A: Vector ( $1^{--}$ ) or Axial ( $1^{++}$ )
- Isospin 1 due to the charge
- Negative G-parity  $\Rightarrow$  positive C-parity

$$\Rightarrow J^{PC} = 1^{++}$$



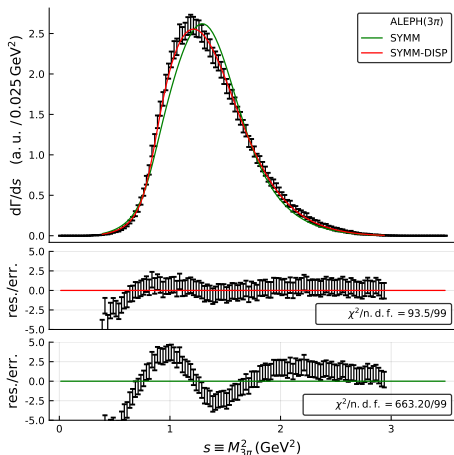
## Fit to ALEPH data

[data from ALEPH, Phys.Rept.421 (2005)]



## Fit to ALEPH data

[data from ALEPH, Phys.Rept.421 (2005)]

Dispersive model vs  
Non-dispersive model

- Difference: LH singularities
- The dispersive model fits significantly better

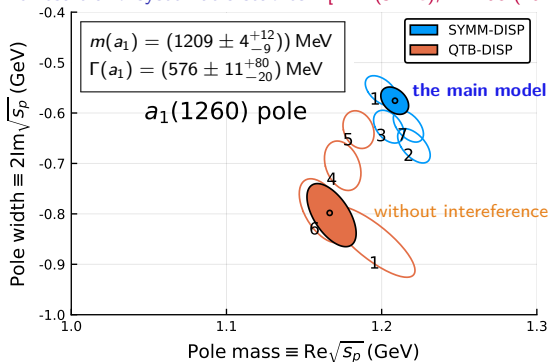
## Fit function

$$\chi^2(c, m, g) = (\vec{D} - \vec{M}(c, m, g))^T C_{\text{stat}}^{-1} (\vec{D} - \vec{M}(c, m, g)),$$

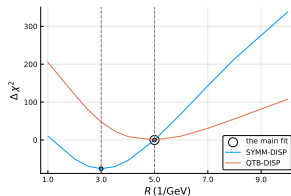
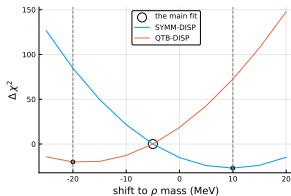
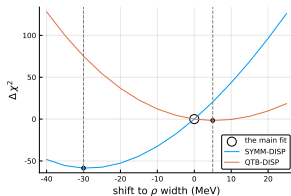
- Stat. cov. matrix is used in the fit
- Syst. cov. matrix – in the bootstrap

# First measurement of the $a_1(1260)$ pole position

The result and systematic studies [MM (JPAC), PRD98 (2018), 096021]



#	Fit studies
1	$s < 2 \text{ GeV}^2$
2	$R' = 3 \text{ GeV}^{-1}$
3	$m'_\rho = m_\rho + 10 \text{ MeV}$
4	$m'_\rho = m_\rho - 10 \text{ MeV}$
5	$m'_\rho = m_\rho - 20 \text{ MeV}$
6	$\Gamma'_\rho = \Gamma_\rho + 5 \text{ MeV}$
7	$\Gamma'_\rho = \Gamma_\rho - 30 \text{ MeV}$



# Summary

## Meson spectroscopy

- Using hadronic scattering as QCD excitation laboratory.
- Mapping gluonic degrees of freedom to structures of excited states is an essential test of QCD.
- Non-perturbative methods are required

## Recent impact of JPAC to light meson spectroscopy

Extensive analyses and extraction of resonance poles:

- Tensor states:  $a_2(1320)$  and  $a_2(1700)$
- Establishing single exotic  $\pi_1(1600)$
- Ground axial state  $a_1(1260)$

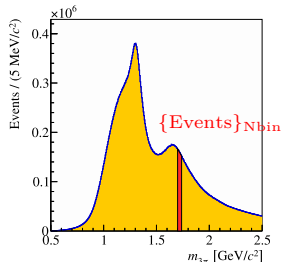
## JPAC effort

- > 50 research papers in PRD, PLB, PRL, EJPC (> 10 in 2018)
- > 100 invited talks and seminars
- Collaboration with GlueX, CLAS12, COMPASS, MAMI, BaBar, LHCb,...
- Summer Schools on Reaction Theory (2015, 2017)

Thank you

# Three-particles PW technique

COMPASS@PWA

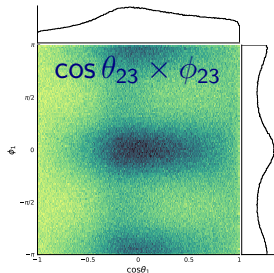
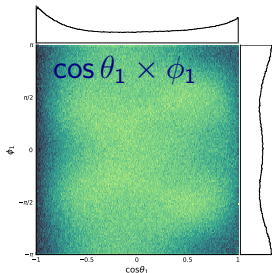
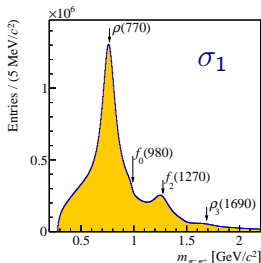


Model: a sum of 88\* partial waves

$$A = c_1 \left( \begin{array}{c} \rho^{++} \\ \rho \\ \pi^+ \pi^- \end{array} \right) + c_2 \left( \begin{array}{c} \rho^{++} \\ \rho \\ \pi^+ \pi^- \end{array} \right) + c_3 \left( \begin{array}{c} f_0 \\ f_2 \\ \pi^+ \pi^- \end{array} \right) + \dots$$

Likelihood Fit: a product of probability per event

$$L = \prod_{e=1}^{N_{events}} \frac{A(\tau_e)}{\int d\tau_e A(\tau_e)}, \quad \tau = (\sigma_1, \cos \theta_1, \phi_1, \cos \theta_{23}, \phi_{23})$$



# Tour to the complex plane

[MM (JPAC), PRD98 (2018), 096021]

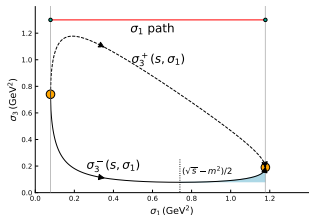
## Analytical continuation

$$|t_I^{-1}(s)| = \left| \frac{m^2 - s}{g^2} - i \left( \frac{\tilde{\rho}(s)}{2} + \rho(s) \right) \right|.$$

- Analytical continuation of  $\rho(s)$ : integral over the Dalitz plot for the complex energy

$$\rho(s) = \sum_{\lambda} \int d\Phi_3 \left| f_{\rho}(\sigma_1) d_{\lambda 0}(\theta_{23}) - f_{\rho}(\sigma_3) d_{\lambda 0}(\hat{\theta}_3 + \theta_{12}) \right|^2$$

- Analytic continuation of  $\rho$ -meson decay amplitude  $f_{\rho}$ 
  - Breit-Wigner amplitude with the dynamic width
  - $P$ -wave Blatt-Weisskopf factors





# Tour to the complex plane

[MM (JPAC), PRD98 (2018), 096021]

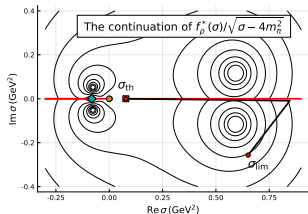
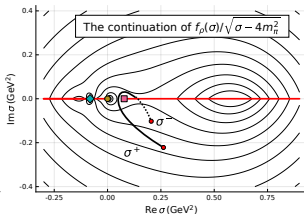
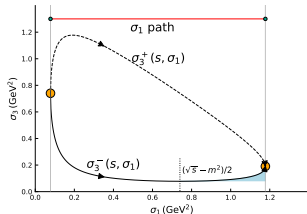
## Analytical continuation

$$|t_I^{-1}(s)| = \left| \frac{m^2 - s}{g^2} - i \left( \frac{\tilde{\rho}(s)}{2} + \rho(s) \right) \right|.$$

- Analytical continuation of  $\rho(s)$ : integral over the Dalitz plot for the complex energy

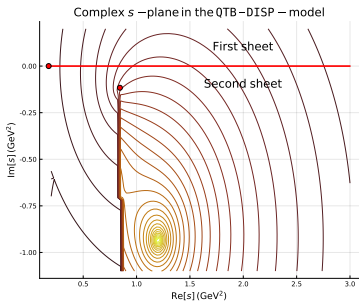
$$\rho(s) = \sum_{\lambda} \int d\Phi_3 \left| f_{\rho}(\sigma_1) d_{\lambda 0}(\theta_{23}) - f_{\rho}(\sigma_3) d_{\lambda 0}(\hat{\theta}_3 + \theta_{12}) \right|^2$$

- Analytic continuation of  $\rho$ -meson decay amplitude  $f_{\rho}$ 
  - Breit-Wigner amplitude with the dynamic width
  - $P$ -wave Blatt-Weisskopf factors



# Tour to the complex plane

[MM (JPAC), PRD98 (2018), 096021]



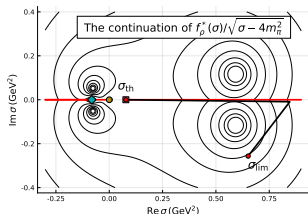
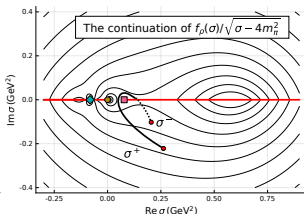
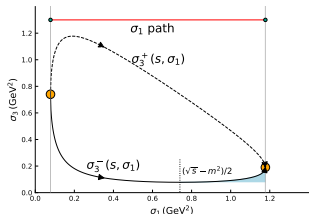
## Analytical continuation

$$|t_{\mathbf{l}}^{-1}(s)| = \left| \frac{m^2 - s}{g^2} - i \left( \frac{\tilde{\rho}(s)}{2} + \rho(s) \right) \right|.$$

- Analytical continuation of  $\rho(s)$ : integral over the Dalitz plot for the complex energy

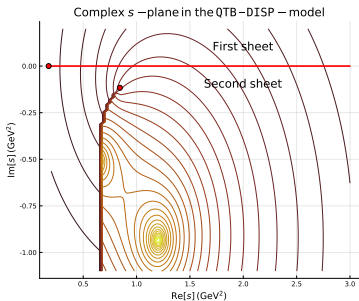
$$\rho(s) = \sum_{\lambda} \int d\Phi_3 \left| f_{\rho}(\sigma_1) d_{\lambda 0}(\theta_{23}) - f_{\rho}(\sigma_3) d_{\lambda 0}(\hat{\theta}_3 + \theta_{12}) \right|^2$$

- Analytic continuation of  $\rho$ -meson decay amplitude  $f_{\rho}$ 
  - Breit-Wigner amplitude with the dynamic width
  - $P$ -wave Blatt-Weisskopf factors



# Tour to the complex plane

[MM (JPAC), PRD98 (2018), 096021]



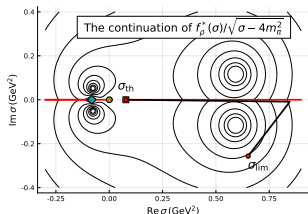
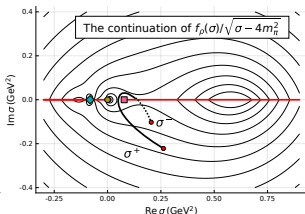
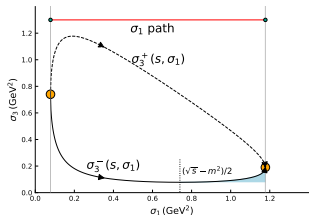
## Analytical continuation

$$|t_l^{-1}(s)| = \left| \frac{m^2 - s}{g^2} - i \left( \frac{\tilde{\rho}(s)}{2} + \rho(s) \right) \right|.$$

- Analytical continuation of  $\rho(s)$ : integral over the Dalitz plot for the complex energy

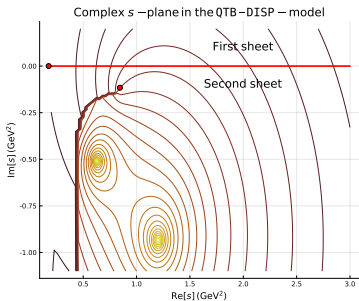
$$\rho(s) = \sum_{\lambda} \int d\Phi_3 \left| f_{\rho}(\sigma_1) d\lambda_0(\theta_{23}) - f_{\rho}(\sigma_3) d\lambda_0(\hat{\theta}_3 + \theta_{12}) \right|^2$$

- Analytic continuation of  $\rho$ -meson decay amplitude  $f_{\rho}$ 
  - Breit-Wigner amplitude with the dynamic width
  - $P$ -wave Blatt-Weisskopf factors



# Tour to the complex plane

[MM (JPAC), PRD98 (2018), 096021]



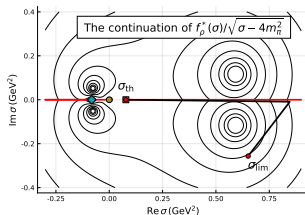
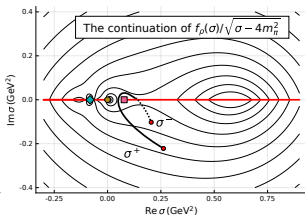
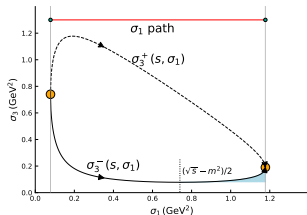
## Analytical continuation

$$|t_l^{-1}(s)| = \left| \frac{m^2 - s}{g^2} - i \left( \frac{\tilde{\rho}(s)}{2} + \rho(s) \right) \right|.$$

- Analytical continuation of  $\rho(s)$ : integral over the Dalitz plot for the complex energy

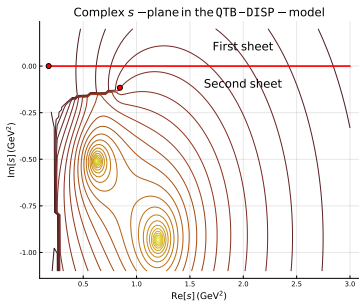
$$\rho(s) = \sum_{\lambda} \int d\Phi_3 \left| f_{\rho}(\sigma_1) d_{\lambda 0}(\theta_{23}) - f_{\rho}(\sigma_3) d_{\lambda 0}(\hat{\theta}_3 + \theta_{12}) \right|^2$$

- Analytic continuation of  $\rho$ -meson decay amplitude  $f_{\rho}$ 
  - Breit-Wigner amplitude with the dynamic width
  - $P$ -wave Blatt-Weisskopf factors



# Tour to the complex plane

[MM (JPAC), PRD98 (2018), 096021]



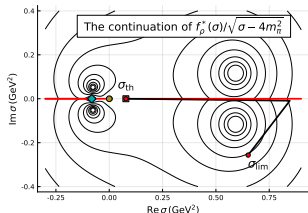
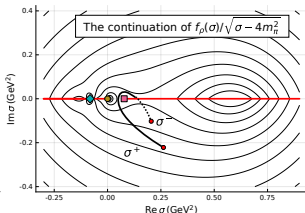
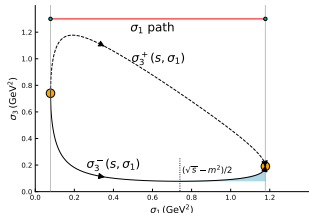
## Analytical continuation

$$|t_l^{-1}(s)| = \left| \frac{m^2 - s}{g^2} - i \left( \frac{\tilde{\rho}(s)}{2} + \rho(s) \right) \right|.$$

- Analytical continuation of  $\rho(s)$ : integral over the Dalitz plot for the complex energy

$$\rho(s) = \sum_{\lambda} \int d\Phi_3 \left| f_{\rho}(\sigma_1) d_{\lambda 0}(\theta_{23}) - f_{\rho}(\sigma_3) d_{\lambda 0}(\hat{\theta}_3 + \theta_{12}) \right|^2$$

- Analytic continuation of  $\rho$ -meson decay amplitude  $f_{\rho}$ 
  - Breit-Wigner amplitude with the dynamic width
  - $P$ -wave Blatt-Weisskopf factors

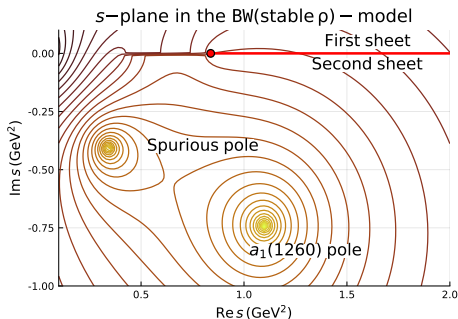


# The spurious pole in the Breit-Wigner model

Energy dependent width, stable particles

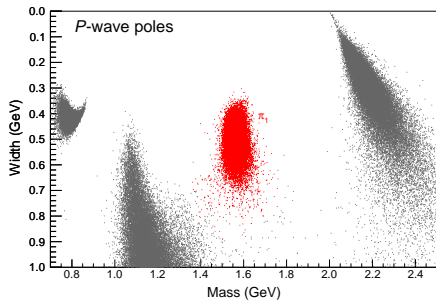
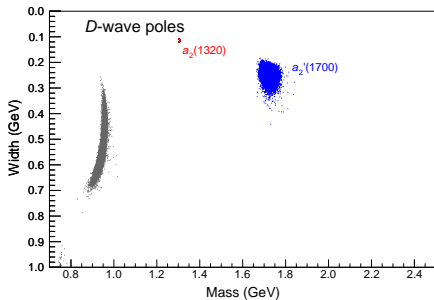
$$t(s) = \frac{1}{m^2 - s - im\Gamma(s)}, \quad \Gamma(s) = \Gamma_0 \frac{p(s)}{p(m^2)} \frac{m}{\sqrt{s}}, \quad p(s) = \frac{\sqrt{(s - (m_1 + m_2)^2)(s - (m_1 - m_2)^2)}}{2\sqrt{s}}.$$

Example:  $m_1 = 140 \text{ MeV}$ ,  $m_2 = 770 \text{ MeV}$ ,  $m = 1.26 \text{ GeV}$ ,  $\Gamma_0 = 0.5 \text{ GeV}$



Live demo

# Bootstrap: stability of the poles



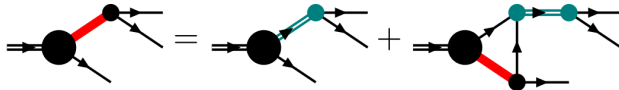
- Statistical bands are obtained by 50k bootstrap samples

# Subchannel dynamics

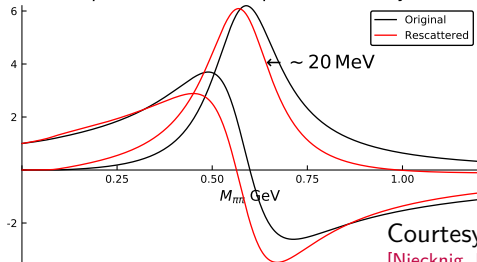
## Khuri-Treiman equations

Consistency equations for the isobar lineshape

- Governed by two-body unitarity
- Model: only RHC for the isobar amplitude
- Uses Analyticity / Cauchy theorem / Omnès trick



$\rho$  – meson lineshape in  $\omega$  – decay



KT analysis of  $\omega \rightarrow 3\pi$

- $\rho \rightarrow \rho$  rescattering
- Solved by iteration

Courtesy of Tobias Isken

[Niecknig, Kubis, JHEP 1510 (2015) 142]